THE JOURNAL OF PHYSICAL CHEMISTRY C

Article

pubs.acs.org/JPCC

Tunable Hybridized Quadrupole Plasmons and Their Coupling with Excitons in ZnMgO/Ag System

Hong-Yu Chen,[†,‡] Ke-Wei Liu,*[,†] Ming-Ming Jiang,[†] Zhen-Zhong Zhang,[†] Lei Liu,[†] Bing-Hui Li,[†] Xiu-Hua Xie,[†,‡] Fei Wang,[†,‡] Dong-Xu Zhao,[†] Chong-Xin Shan,[†] and De-Zhen Shen*[,†]

[†]State Key Laboratory of Luminescence and Applications, Changchun Institute of Optics, Fine Mechanics and Physics, Chinese Academy of Sciences, Dongnanhu Road 3888, Changchun, 130033, People's Republic of China

[‡]Graduate University of the Chinese Academy of Sciences, Beijing, 100049, People's Republic of China

Supporting Information

ABSTRACT: The tunable hybridized quadrupole plasmons and their strong coupling with excitons have been demonstrated in ZnMgO/Ag nanoclusters (NCs) system. By adjusting the density of the random Ag NCs, the hybridized quadrupole resonance with strong intensity can be obtained due to the asymmetry Fano-like interference. Owing to a good energy match between hybridized quadrupole plasmons and excitons of ZnMgO, a giant near-band-edge UV emission enhancement was realized. The finite difference time-domain method was used to demonstrate the formation of the tunable hybridized quadrupole resonance in the short wavelength range. This novel method for enhancing the UV emission, associated with the hybridized quadrupole plasmons, may pave the way for the further development of high-efficiency UV light-emitting diodes and laser diodes.

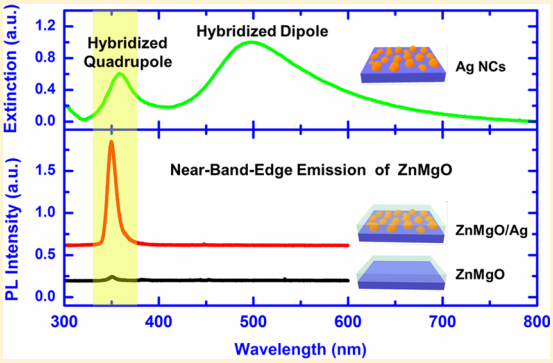

INTRODUCTION

Ultraviolet (UV) light-emitting materials and devices with high efficiency are required for many applications, such as optical storage, optical communication, environmental protection, and so forth.[1,2] Owing to its unique merit of concentrating and manipulating the light at the subwavelength scale, plasmonics is an effective scheme for enhancing the luminescence efficiency, which has been widely investigated for this purpose in the last two decades.[3−10] To achieve giant enhancement of UV luminescence by surface plasmons, the key factor is their energy match, namely the large frequency overlap between surface plasmons and UV emissions.[4,7,10] According to the previous reports, dipole resonance is the most easily realized mode among the surface plasmon resonance modes and can couple directly with the incident light.[4,10,11] However, the dipole resonance frequency is usually far away from the UV range, which cannot satisfy the energy matching requirement. Although its resonance frequency could be blue shifted via reducing the size of the metallic nanostructures, extending it into the UV range experimentally is still beyond the current nanofabrication techniques. Moreover, according to the Mie theory, the small nanoparticles have weaker scattering intensity and a lower integrated scattering/absorption cross-section ratio that will limit the UV light enhancement.[12−15] Therefore, the direct realization of UV light enhancement by the traditional dipolar plasmon mode is still challenging. High-order multipoles excited in the short wavelength regime should satisfy the requirements of energy match for UV emission enhancement. However, multipoles are usually damped and overlap with dipole mode, so that their influence on emission is relatively minor. Recently, it is found that the multipolar resonance can be separately obtained in larger size or higher asymmetry metallic nanostructures.[16−18] More interestingly, the multipolar resonance, such as quadrupole, could tailor the UV light emission, that is, the modification of the exciton recombination rate in ZnO/ZnMgO quantum-well heterostructures and the enhancement of the band-edge emission from ZnO.[19,20] It confirms that the quadrupole modes as the darkness state do not always produce the luminescence quenching effect but can be used to enhance the UV light emission.[21] However, the coupling between quadrupole and UV light emission suffers from the lower intensity of primitive quadrupole resonance. Hence, the ability to improve the quadrupole resonance intensity is urgently required, which will be benefit for the UV light emission enhancement. According to the previous reports, the Fano interference in the Ag nanoparticle aggregations could strongly influence the intensity of quadrupole resonance: either enhancement or suppression.[22−26] Therefore, a significant hybridized quadrupole mode is expected to be realized by tuning the coupling interaction in the nanostructrued metallic systems, which in turn results in a giant UV emission enhancement. So far, most research focused on the profile of the extinction spectra in different nanostructrued metallic systems[25−29] but enhancing the UV

Received: November 14, 2013
Revised: December 14, 2013
Published: December 16, 2013

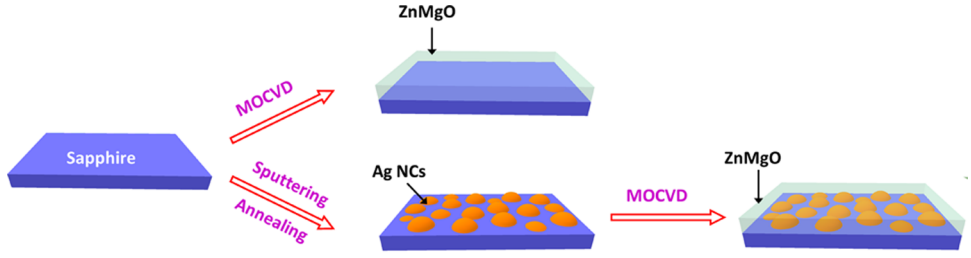

Figure 1. Schematic diagram of the fabrication processing of samples (ZnMgO/Ag) and reference sample (ZnMgO).

emission by the hybridized quadrupole associated with the plasmonic interference has not been explored.

In this article, we demonstrate a giant enhancement of UV light emission by the strong coupling between hybridized quadrupole plasmons and excitons in ZnMgO/Ag system. ZnMgO was selected as the UV emission material due to its excellent optical properties and potential applications in UV light-emitting diodes (LEDs), photodetectors, and laser diodes.[30−33] The random Ag nanoclusters (NCs) were fabricated by a very simple sputtering method without any sophisticated lithography processes, which will be benefit for the future practical applications. The observed quadrupole in our random Ag NCs mainly consists of the hybridized quadrupole induced by the Fano-like interference among the neighboring nanoparticles as well as the primitive quadrupole of isolated Ag nanoparticles with larger size. Interestingly, the hybridized quadrupole mode in our Ag NCs, gaining the sufficient intensity by the dipole−quadrupole interference, could result in a giant enhancement of near-band-edge (NBE) emission from ZnMgO by a strong coupling between hybridized quadrupole plasmons and excitons. The experimental results are in good agreement with the finite difference time-domain (FDTD) simulation results, which shed light on the nature of the underlying physics.

EXPERIMENTAL SECTION

The fabrication process of the ZnMgO/Ag NCs system is shown in Figure 1. Ag (99.99%) was deposited on the c-face sapphire by a radio frequency magnetron sputtering technique at room temperature, subsequently annealed in N_2 atmosphere at 450 °C to form Ag NCs. After that, ∼200 nm thick hexagonal ZnMgO films were deposited by metal−organic chemical vapor deposition (MOCVD) at 450 °C, and the chamber pressure was kept at 2×10^4 Pa. Oxygen (99.999%), diethylzinc (DEZn), and dimethyl dicyclopentadienyl magnesium ($(MeCp)_2Mg$) were employed as the precursors and nitrogen (99.999%) was used as the carrier gas.

The morphology of the samples was characterized by scanning electron microscope (SEM). The extinction spectra were measured by a Shimadzu UV-3101PC scanning spectrophotometer. An energy-dispersive X-ray spectrometer (EDS) was used to evaluate the composition of the ZnMgO thin films. Temperature-dependent photoluminescence (PL) measurement was characterized using an SPEX 1404 spectrometer in a close-cycled He cryostat between 12 and 300 K with a 224 nm He−Ag pulsed laser

RESULTS AND DISCUSSION

The extinction spectra of Ag NCs with the different sputtering times ranging from 6 to 12 min and the corresponding scanning electron microscope (SEM) images are shown in Figure 2.

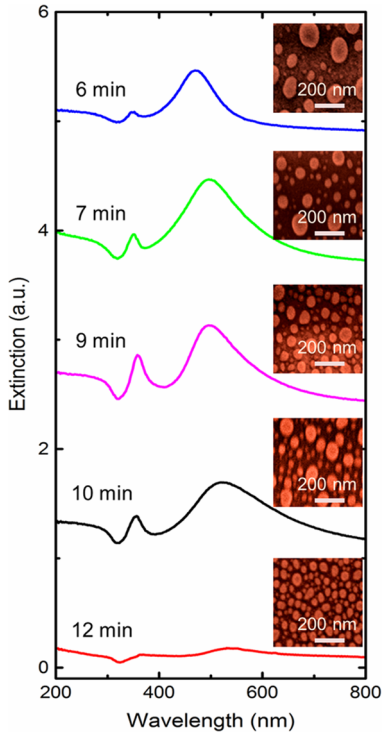

Figure 2. Extinction spectra of Ag NCs sputtered on the c-plane sapphire with different sputtering times of 6, 7, 9, 10, and 12 min. The right insets are the corresponding SEM images.

From the SEM images, it is evident that the diameter of Ag nanoparticles varies from 30 to 100 nm, and the density of Ag NCs increases with the increase in the sputtering time. In the extinction spectra, all samples exhibit two peaks clearly: one is located at visible range and another is located at UV range. The visible extinction peak dramatically red shifts with increasing the sputtering time. As for the UV extinction peak, it first gains significant intensity when we increase the sputtering time from 6 to 9 min, but the intensity decreases with further increasing the sputtering time. Meanwhile, the UV extinction peak does not shift appreciably. Notablely, a unique asymmetric profile was observed for Ag NCs with the sputtering time of 6, 7, 9, and 10 min, which is well-known as Fano-like profile. In this work, the special profiles in extinction spectra could be mainly attributed to the coupling interaction between dipole and quadrupole of Ag NCs. Thus, the extinction peaks located at visible and UV ranges of Ag NCs with the sputtering time of 6, 7, 9, and 10 min should correspond to the hybridized dipole and quadrupole modes, respectively. Additionally, the primitive modes in isolated Ag nanoparticles can not be excluded in our random system, especially in lower density one. Usually, dark quadrupole modes cannot be optically excited directly from the

dx.doi.org/10.1021/jp411218v | J. Phys. Chem. C 2014, 118, 679−684

far-field under plane wave illumination. However, it can be excited by the near-field associated with the bright dipole mode. Hence, the illumination field first excites the bright mode, which then excites the dark mode in our case.[34,35] In addition, the asymmetry profile shows an obvious red shift and the hybridized quadrupole is enhanced with the sputtering time increasing from 6 to 9 min due to the increase in dipole−quadrupole interactions. With further increase in the sputtering time, the intensity of hybridized quadrupole resonance decreases. As for the 12 min Ag NCs, the extinction peaks are very weak and appear more as distinct peaks instead of as Fano-like resonance due to its quasi-continuous nature as shown in the right inset of Figure 2. This phenomenon could be explained by the fact that the density of Ag NCs increases with the increase in sputtering time, resulting in a transformation from the localized surface plasmon polarizations (LSPPs) to the delocalized surface plasmon polarizations (DSPPs).[36] Therefore, it can be concluded that the hybridized plasmon state could be tailored by varying the density of Ag NCs.

To test the effect of plasmonic quadrupole Fano-like resonance on the UV emission, ZnMgO films were deposited on Ag NCs with the sputtering time of 6, 9, and 12 min by MOCVD to form ZnMgO/Ag NCs, which are labeled as B, C, and D, respectively. The PL spectra of samples B−D and the reference sample A (bare ZnMgO without Ag NCs) were measured at different temperatures. Bare ZnMgO exhibits a strong UV emission at low temperature, but the PL signal could be neglected above 120 K (see Supporting Information Figure S1). Figure 3a shows the PL spectra of all samples measured at 50 K. Only one UV peak was observed for all samples, which is attributed to the NBE emission of ZnMgO, and no visible emission associated with defects could be found. The NBE emission peaks of samples A, B, C, and D are located at 350.2, 346.1, 349.8, and 355.8 nm, respectively. Notablely, compared with that of bare ZnMgO (Sample A), the NBE emission peaks of samples B and C shift to the blue side and the intensity increases a lot. As for sample D, its PL intensity is comparable with that of bare ZnMgO and the peak shows a slight red shift. The change in PL spectra should be the results of coupling between the NBE emissions from ZnMgO and Ag NCs plasmons. According to the previous reports, the dipole modes could be responsible for the large UV emission enhancement of samples B and C.[4,10,11] However, considering that the hybridized dipole frequency of Ag NCs (6 min) has a better match with ZnMgO NBE emission than that of Ag NCs (9 min) (see Figure 2), the PL intensity of sample B should be stronger than that of sample C. Additionally, the hybridized dipole with lower frequency should realize the red shift of the NBE UV emission of ZnMgO. All of these are not consistent with our experimental results. Therefore, the contribution of hybridized dipole modes to the emission enhancement can be neglected in our case.

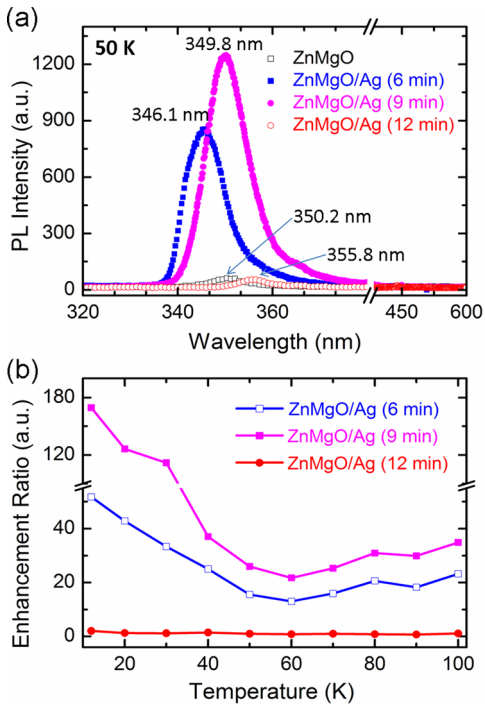

Figure 3. (a) PL spectra of bare ZnMgO, ZnMgO/Ag (6 min), ZnMgO/Ag (9 min), and ZnMgO/Ag (12 min) measured at 50 K. (b) PL enhancement ratio as a function of temperature from 12 to 100 K for different samples. The PL enhancement ratio is defined as the integrated PL intensity of the hybrid sample with respect to that of the bare ZnMgO film.

By comparing the PL spectra in Figure 3a to the extinction spectra in Figure 2, it is found that the NBE emission peak intensity as a function of Ag sputtering time shows a similar trend with that of the hybridized quadrupole resonance. Thus, we conclude that the coupling between NBE emission and the hybridized quadrupole modes is the main reason for the giant PL enhancement. The difference in enhancement ratios between samples B and C can be explained by the different hybridized quadrupole resonance intensities. As for sample D, its neglectable PL enhancement was mainly caused by the weak quadrupole resonance.

To better understand the enhancement of UV emission by the hybridized quadrupole, the integrated PL intensity of the hybrid sample with respect to that of the bare ZnMgO film, the PL enhancement ratio, is plotted as a function of measurement temperature from 12 to 100 K, as shown in Figure 3b. It can be seen that the enhancement ratio of sample D is very small (below 2) and nearly constant over the whole temperature range due to its weak quadrupole resonance. As for samples B and C, the enhancement ratio increases with decreasing temperature. Notablely, owing to the strongest quadrupolar resonances of Ag NCs and a very good spectra match with ZnMgO NBE emission, the enhancement ratio of sample C can reach a value as high as 170 at 12 K. The enhanced ratio does not increase monotonically with decreasing the temperature due to the complex interactions among excitons, hybridized plasmons, and phonons. In addition, the PL enhancement effect of all samples is very stable for at least several months.

As we mentioned above, the hybridized quadrupole resonance with strong intensity was the key factor for the giant UV light enhancement via the plasmons-excitons coupling. To further demonstrate the origin of the hybridized quadrupole in the Ag NCs system and the mechanism of NBE emission enhancement from ZnMgO film, FDTD simulations were carried out. The theoretical extinction spectra of the isolate Ag nanosphere based on the optical constants measured by Johnson and Christy are shown in Figure 4a.[11,37] In the extinction spectra, the peaks at ~500 and ~350 nm could be assigned to the dipole and quadrupole plasmon resonance, respectively, which are calculated by the Mie theory.[11,18,20] It can be found that the quadrupole plasmon resonance appears

dx.doi.org/10.1021/jp411218v | J. Phys. Chem. C 2014, 118, 679−684

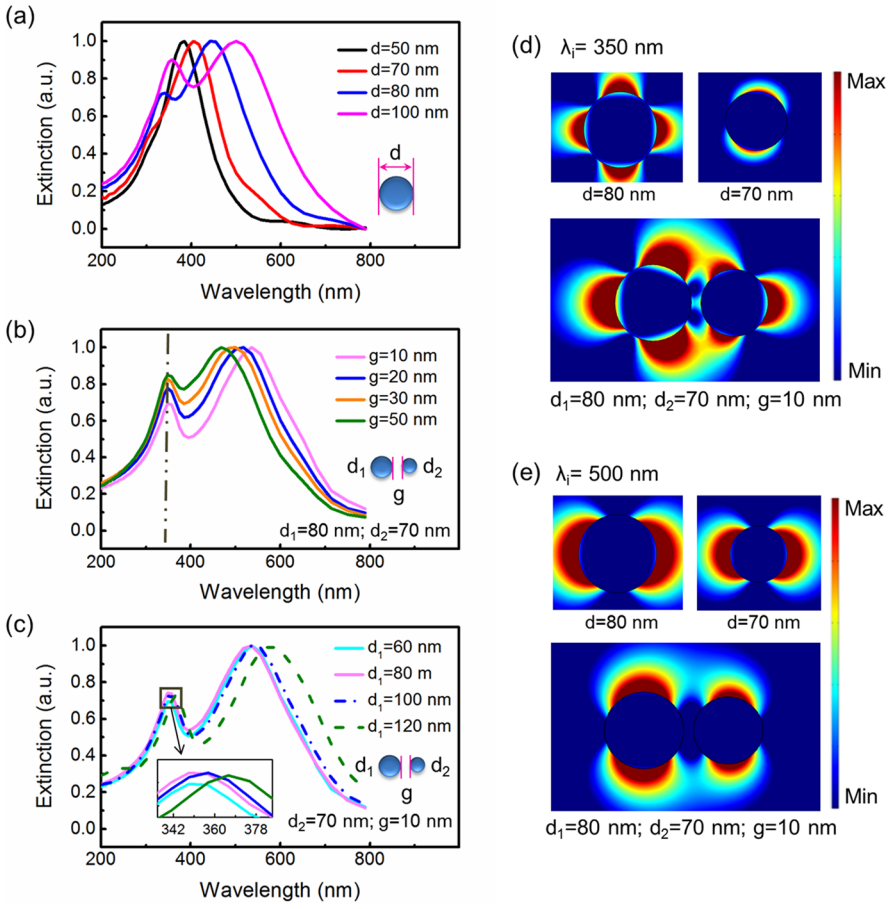

Figure 4. Extinction spectra and the spatial distribution of the electric field obtained by FDTD simulation. (a) Extinction spectra of the isolated nanospheres with d = 50, 70, 80, and 100 nm. (b) Extinction spectra of the dimer with internal gap g = 10, 20, 30, and 50 nm. The diameters of two nanospheres d_1 and d_2 are fixed at 80 and 70 nm, respectively. (c) Extinction spectra of the dimer with one nanosphere diameter d_1 = 60, 80, 100, and 120 nm. Another nanosphere diameter d_2 and the internal gap g are fixed at 70 and 10 nm, respectively. (d,e) Spatial distribution of the electric field intensity at the wavelength of 350 and 500 nm. In all simulations, the direction of the incident light is perpendicular to the electric field distribution plane.

and becomes obvious in the UV regime with increasing the diameter of nanosphere. The quadrupole mode is mainly induced by the inhomogeneous charge distribution in the nanosphere.[18] Considering the random dispersion of Ag NCs in our experiment, we simulate the coupling interaction in a simple dimer unit to evaluate the collective effect of all NCs. As is well-known, plasmon coupling interaction between two Ag nanospheres is sensitive to their diameters (d) and internal gap (g). To investigate the formation of the tunable hybridized quadrupole in the short wavelength region, the extinction spectra of plasmonic dimer clusters were calculated using FDTD as shown in Figure 4b,c. In Figure 4b, the diameters of two nanospheres are kept at constant (d_1 = 80 nm, d_2 = 70 nm), and the simulated extinction spectra of the dimers as a function of g are presented. It can be found that the profile of extinction spectra becomes more asymmetrical with g decreasing from 50 to 10 nm; the intensity of quadrupole resonances of the dimer becoming stronger and the Fano-like dips becoming deeper. This trend is mainly derived from the increase in the coupling strength with decreasing g. Meanwhile, the frequency of the hybridized quadrupole resonance shows almost no change with the decrease in g, while the hybridized dipole plasmon resonance red shifts. Besides the internal gap, the plasmon coupling can also be tuned by adjusting the diameter of the nanospheres in dimer, and the calculated extinction spectra of the dimers with g = 10 nm, d_2 = 70 nm, and d_1 = 60−120 nm are shown in Figure 4c. With increasing d_1 from 60 to 120 nm, an obvious frequency redshift of the hybridized quadrupole can be observed, while size effect on the coupling interaction of nanoparticles is very small. In order to describe the plasmon coupling more clearly, the electric field spatial distribution $E(x, y)$ of the dimer (with d_1 = 80 nm, d_2 = 70 nm and g = 10 nm) was simulated at the wavelength of 350 and 500 nm (see Figure 4d,e). The coupling interaction between two nanospheres in the short wavelength region results in asymmetry breaking of the charge distribution within the nanospheres, which is the origin of the hybridized quadrupole in this work.[24−29,38,39] Therefore, the simulated extinction spectra and the electric field distribution of the dimer indicate that the intensity of the hybridized quadrupole is highly sensitive to the internal gap, and the diameter of nanospheres could affect the frequency of the hybridized quadrupole.

Although a simple dimer in the simulation can not directly describe the random Ag NCs in our experiment, it does not affect the understanding of the formation of the tunable hybridized quadrupole resonance in our random Ag NCs. The experimental results can be well explained by the simulation results. In our experiment, Ag nanoparticles have a diameter of 30−120 nm, and the average internal gap decreases with the

dx.doi.org/10.1021/jp411218v | J. Phys. Chem. C 2014, 118, 679−684

increase in the sputtering time (see Figure 2). For the Ag NCs with the sputtering time less than 6 min, the average internal gap is larger than 60 nm and most Ag nanoparticles are isolated from each other. The quadrupole was dominated by the primitive quadrupole in isolated larger Ag nanoparticles. With increasing the sputtering time, the average internal gap decreases and the coupling strength among the nanoparticles increases. Then, the hybridized quadrupole with strong intensity can be induced by the coupling interactions among nanoparticles. When the sputtering time is more than 12 min, the average internal gap decreased sharply and the Ag nanoparticles became continuous, resulting in the weakening or disappearance of the quadrupole resonance.

As for the strong NBE emission enhancement in ZnMgO/Ag NCs system, the main reason should be the strong hybridized quadruple plasmons induced by dipole−quadrupole Fano-like interference among nanoparticles. This asymmetry interference could lead to a large enhancement of electromagnetic field between the neighboring particles,[22,28] as well as a big increase in the local density of optical states for radiation at the same wavelength.[8,9,27,40−43] Owing to the good energy match between the hybridized quadrupole mode and NBE excitons in ZnMgO, the radiative recombination rate of excitons is enhanced by surface plasmon resonance.[4−11] Thus, high-efficiency ZnMgO NBE emission can be indeed achieved by a strong coupling between the hybridized quadrupole plasmons and excitons.

CONCLUSIONS

In summary, we experimentally and theoretically demonstrate a tunable hybridized quadrupole plasmons and their coupling with excitons in ZnMgO/Ag NCs system. The hybridized quadrupole resonances, induced by the interaction between dipole and quadrupole resonance modes in short wavelength region, can be controlled by simply turning the density of the random Ag NCs. Because of their large frequency overlap between hybridized quadrupole and excitons, a giant enhancement of NBE emission from ZnMgO in this hybrid architecture was obtained. Our results should stimulate future studies on the viewpoints of both fundamental science and device applications. This novel method for enhancing the UV emission may pave the way for the further development of high-performances LEDs, laser diodes, and photodetectors, as well as other semiconductor devices in the short wavelength regime.[44−47]

ASSOCIATED CONTENT

Supporting Information

Additional experimental details including the PL spectra and EDS results of MgZnO/Ag. This material is available free of charge via the Internet at http://pubs.acs.org.

AUTHOR INFORMATION

Corresponding Authors

*E-mail: (K.-W.L.) liukw@ciomp.ac.cn.
*E-mail: (D.-Z.S.) shendz@ciomp.ac.cn.

Notes

The authors declare no competing financial interest.

ACKNOWLEDGMENTS

This work is supported by the National Basic Research Program of China (973 Program) (Nos. 2011CB302006, 2011CB302004), the National Natural Science Foundation of China (Nos. 10974197, 11174273, 11104265, 21101146), the 100 Talents Program of the Chinese Academy of Sciences.

REFERENCES

(1) Xu, Z.; Sadler, B. M. Ultraviolet Communications: Potential and State-of-The-Art. *IEEE Commun. Mag.* **2008**, *46*, 67−73.
(2) Taniyasu, Y.; Kasu, M.; Makimoto, T. An Aluminium Nitride Light-Emitting Diode with A Wavelength of 210 Nanometres. *Nature* **2006**, *441*, 325−328.
(3) Quidant, R.; Girard, C. Surface-Plasmon-Based Optical Manipulation. *Laser Photonics Rev.* **2008**, *2*, 47−57.
(4) Okamoto, K.; Niki, I.; Shvartser, A.; Narukawa, Y.; Mukai, T.; Scherer, A. Surface-Plasmon-Enhanced Light Emitters Based on InGaN Quantum Wells. *Nat. Mater.* **2004**, *3*, 601−605.
(5) Ding, K.; Ning, C. Metallic Subwavelength-Cavity Semiconductor Nanolasers. *Light: Sci. Appl.* **2012**, *1*, e20.
(6) Liu, K. W.; Tang, Y D.; Cong, C. X.; Sum, T. C.; Huan, A. C. H.; Shen, Z. X; Wang, L.; Jiang, F. Y; Sun, X. W.; Sun, H. D. Giant Enhancement of Top Emission From ZnO Thin Film by Nano-patterned Pt. *Appl. Phys. Lett.* **2009**, *94*, 151102.
(7) Okamoto, K.; Niki, I.; Scherer, A.; Narukawa, Y.; Mukai, T.; Kawakami, Y. Surface Plasmon Enhanced Spontaneous Emission Rate of InGaN/GaN Quantum Wells Probed by Time-Resolved Photo-luminescence Spectroscopy. *Appl. Phys. Lett.* **2005**, *87*, 071102.
(8) Schuller, J. A.; Barnard, E. S.; Cai, W.; Jun, Y. C.; White, J. S.; Brongersma, M. L. Plasmonics for Extreme Light Concentration and Manipulation. *Nat. Mater.* **2010**, *9*, 193−204.
(9) Ma, R. M.; Oulton, R. F.; Sorger, V. J.; Zhang, X. Plasmon Lasers: Coherent Light Source at Molecular Scales. *Laser Photonics Rev.* **2013**, *7*, 1−21.
(10) Cheng, P.; Li, D.; Yuan, Z.; Chen, P.; Yang, D. Enhancement of ZnO Light Emission via Coupling With Localized Surface Plasmon of Ag Island Film. *Appl. Phys. Lett.* **2008**, *92*, 041119.
(11) Maier, S. A. *Plasmonics: Fundamentals and Application*; Springer: New York, 2007.
(12) Scholl, J. A.; Koh, A. L.; Dionne, J. A. Quantum Plasmon Resonances of Individual Metallic Nanoparticles. *Nature* **2012**, *483*, 421−427.
(13) Rycenga, M.; Cobley, C. M.; Zeng, J.; Li, W.; Moran, C. H.; Zhang, Q.; Qin, D.; Xia, Y. Controlling the Synthesis and Assembly of Silver Nanostructures for Plasmonic Applications. *Chem. Rev.* **2011**, *111*, 3669−3712.
(14) Oulton, R. F. Plasmonics: Loss and Gain. *Nat. Photonics* **2012**, *6*, 219−221.
(15) Pelton, M.; Aizpurua, J.; Bryant, G. Metal-Nanoparticle Plasmonics. *Laser Photonics Rev.* **2008**, *2*, 136−159.
(16) Sau, T. K.; Rogach, A. L.; Jäckel, F.; Klar, T. A.; Feldmann, J. Properties and Applications of Colloidal Nonspherical Noble Metal Nanoparticles. *Adv. Mater.* **2010**, *22*, 1805−1825.
(17) Jin, R.; Cao, Y.; Mirkin, C. A.; Kelly, K.; Schatz, G. C.; Zheng, J. Photoinduced Conversion of Silver Nanospheres to Nanoprisms. *Science* **2001**, *294*, 1901−1903.
(18) Noguez, C. Surface Plasmons on Metal Nanoparticles: The Influence of Shape and Physical Environment. *J. Phys. Chem. C* **2007**, *111*, 3806−3819.
(19) Lawrie, B. J.; Kim, K.-W.; Norton, D. P.; Haglund, R. F., Jr Plasmon-Exciton Hybridization in ZnO Quantum-Well Al Nanodisc Heterostructures. *Nano Lett.* **2012**, *12*, 6152−6157.
(20) Zang, Y.; He, X.; Li, J.; Yin, J.; Li, K.; Yue, C.; Wu, Z.; Wu, S.; Kang, J. Band Edge Emission Enhancement by Quadrupole Surface Plasmon-Exciton Coupling Using Direct-Contact Ag/ZnO Nano-spheres. *Nanoscale* **2013**, *5*, 574−580.
(21) Maier, S. A. The Benefits of Darkness. *Nat. Mater.* **2009**, *8*, 699−700.
(22) Rahmani, M.; Luk'yanchuk, B.; Hong, M. Fano Resonance in Novel Plasmonic Nanostructures. *Laser Photonics Rev.* **2013**, *7*, 329−349.
(23) Zhang, S.; Bao, K.; Halas, N. J.; Xu, H.; Nordlander, P. Substrate-Induced Fano Resonances of A Plasmonic Nanocube: A

Route to Increased-Sensitivity Localized Surface Plasmon Resonance Sensors Revealed. *Nano Lett.* **2011**, *11*, 1657−1663.
(24) Halas, N. J.; Lal, S.; Link, S.; Chang, W. S.; Natelson, D.; Hafner, J. H.; Nordlander, P. A Plethora of Plasmonics from the Laboratory for Nanophotonics at Rice University. *Adv. Mater.* **2012**, *24*, 4842−4877.
(25) Luk'yanchuk, B.; Zheludev, N. I.; Maier, S. A.; Halas, N. J.; Nordlander, P.; Giessen, H.; Chong, C. T. The Fano Resonance in Plasmonic Nanostructures and Metamaterials. *Nat. Mater.* **2010**, *9*, 707−715.
(26) Yang, Z.-J.; Zhang, Z.-S.; Zhang, L.-H.; Li, Q.-Q.; Hao, Z.-H.; Wang, Q.-Q. Fano Resonances in Dipole-Quadrupole Plasmon Coupling Nanorod Dimers. *Opt. Lett.* **2011**, *36*, 1542−1544.
(27) Frimmer, M.; Coenen, T.; Koenderink, A. F. Signature of A Fano Resonance in A Plasmonic Metamolecule's Local Density of Optical States. *Phys. Rev. Lett.* **2012**, *108*, 077404.
(28) Sancho-Parramon, J.; Bosch, S. Dark Modes and Fano Resonances in Plasmonic Clusters Excited by Cylindrical Vector Beams. *ACS Nano* **2012**, *6*, 8415−8423.
(29) Lassiter, J. B.; Sobhani, H.; Knight, M. W.; Mielczarek, W. S.; Nordlander, P.; Halas, N. J. Designing and Deconstructing the Fano Lineshape in Plasmonic Nanoclusters. *Nano Lett.* **2012**, *12*, 1058−1062.
(30) Zhu, H.; Shan, C. X.; Yao, B.; Li, B. H.; Zhang, J. Y.; Zhang, Z. Z.; Zhao, D. X.; Shen, D. Z.; Fan, X. W.; Lu, Y. M. Ultralow-threshold Laser Realized in Zinc Oxide. *Adv. Mater.* **2009**, *21*, 1613−1617.
(31) Xie, X. H.; Zhang, Z. Z.; Shan, C. X.; Chen, H. Y.; Shen, D. Z. Dual-Color Ultraviolet Photodetector Based on Mixed-Phase-MgZnO/i-MgO/P-Si Double Heterojunction. *Appl. Phys. Lett.* **2012**, *101*, 081104.
(32) Liu, K. W.; Sakurai, M.; Liao, M. Y.; Aono, M. Giant Improvement of the Performance of ZnO Nanowire Photodetectors by Au Nanoparticles. *J. Phys. Chem. C* **2010**, *114*, 19835−19839.
(33) Liu, L.; Xu, J. L.; Wang, D. D.; Jiang, M. M; Wang, S. P.; Li, B. H.; Zhang, Z. Z.; Zhao, D. X.; Shan, C. X.; Yao, B. P-type Conductivity in N-doped ZnO: the Role of the N_{zn}-V_o Complex. *Phys. Rev. Lett.* **2012**, *108*, 215501.
(34) Mukherjee, S.; Sobhani, H.; Lassiter, J. B.; Bardhan, R.; Nordlander, P.; Halas, N. J. Fanoshells: Nanoparticles with Built-in Fano Resonances. *Nano Lett.* **2010**, *10*, 2694−2701.
(35) Miroshnichenko, A. E.; Kivshar, Y. S. Fano Resonances in All-dielectric Oligomers. *Nano Lett.* **2012**, *12*, 6459−6463.
(36) Stockman, M. I.; Faleev, S. V.; Bergman, D. J. Localization Versus Delocalization of Surface Plasmons in Nanosystems: Can One State Have Both Characteristics? *Phys. Rev. lett.* **2001**, *87*, 167401.
(37) Johnson, P. B.; Christy, R.-W. Optical Constants of the Noble Metals. *Phys. Rev. B* **1972**, *6*, 4370.
(38) Prodan, E.; Radloff, C.; Halas, N.; Nordlander, P. A Hybridization Model for the Plasmon Response of Complex Nanostructures. *Science* **2003**, *302*, 419−422.
(39) Fan, J. A.; Wu, C.; Bao, K.; Bao, J.; Bardhan, R.; Halas, N. J.; Manoharan, V. N.; Nordlander, P.; Shvets, G.; Capasso, F. Self-Assembled Plasmonic Nanoparticle Clusters. *Science* **2010**, *328*, 1135−1138.
(40) Zuloaga, J.; Nordlander, P. On the Energy Shift between Near-field and Far-field Peak Intensities in Localized Plasmon Systems. *NanoLett.* **2011**, *11*, 1280−1283.
(41) Ye, J.; Wen, F.; Sobhani, H.; Lassiter, J. B.; Dorpe, P. V.; Nordlander, P.; Halas, N. J. Plasmonic Nanoclusters: Near Field Properties of the Fano Resonance Interrogated with SERS. *Nano Lett.* **2012**, *12*, 1660−1667.
(42) Niu, L.; Zhang, J. B.; Fu, Y. H.; Kulkarni, S.; Lukyanchuk, B. Fano Resonance in Dual-Disk Ring Plasmonic Nanostructures. *Opt. Express* **2011**, *19*, 22974−22981.
(43) Lassiter, J. B.; Sobhani, H.; Knight, M. W.; Mielczarek, W. S.; Nordlander, P.; Halas, N. J. Designing and Deconstructing the Fano Lineshape in Plasmonic Nanoclusters. *Nano Llett.* **2012**, *12*, 1058−1062.
(44) Liu, K. W.; Sakurai, M.; Aono, M. Enhancing the Humidity Sensitivity of Ga_2O_3/SnO_2 Core/Shell Microribbon by Applying Mechanical Strain and its Application as a Flexible Strain Sensor. *Small* **2012**, *8*, 3599−3604.
(45) Su, Y.-H.; Ke, Y.-F.; Cai, S.-L.; Yao, Q.-Y. Surface Plasmon Resonance of Layer-by-Layer Gold Nanoparticles induced Photo-electric Current in Environmentally-Friendly Plasmon-Sensitized Solar Cell. *Light: Sci. Appl.* **2012**, *1*, e14.
(46) Liu, K. W.; Sakurai, M.; Aono, M. Controlling Semiconducting and Insulating States of SnO_2 Reversibly by Stress and Voltage. *ACS Nano* **2012**, *6*, 7209−7215.
(47) Liu, M.; Lee, T.-W.; Gray, S. K.; Guyot-Sionnest, P.; Pelton, M. Excitation of Dark Plasmons in Metal Nanoparticles by a Localized Emitter. *Phys. Rev. Lett.* **2009**, *102*, 107401.